

UV–Vis, NMR, and Time-Resolved Spectroscopy Analysis of Photoisomerization Behavior of Three- and Six-Azobenzene-Bound Tris(bipyridine)cobalt Complexes

Kyoko Yamaguchi,[†] Shoko Kume,[†] Kosuke Namiki,[†] Masaki Murata,[†] Naoto Tamai,[‡] and Hiroshi Nishihara^{*†}

Department of Chemistry, School of Science, The University of Tokyo, Hongo, Bunkyo-ku, Tokyo 113-0033, Japan, and Department of Chemistry, Faculty of Science, Kwansai Gakuin University, 2-1 Gakuen, Sanda, Hyogo 669-1337, Japan

Received August 8, 2005

The photoisomerization properties of tris(bipyridine)cobalt complexes containing six or three azobenzene moieties, namely, $[\text{Co}^{\text{II}}(\text{dmAB})_3](\text{BF}_4)_2$ {dmAB = 4,4'-bis[3''-(4'''-tolylazo)phenyl]-2,2'-bipyridine}, $[\text{Co}^{\text{III}}(\text{dmAB})_3](\text{BF}_4)_3$, $[\text{Co}^{\text{II}}(\text{mAB})_3](\text{BF}_4)_2$ {mAB = 4-[3''-(4'''-tolylazo)phenyl]-2,2'-bipyridine}, and $[\text{Co}^{\text{III}}(\text{dmAB})_3](\text{BF}_4)_3$, derived from the effect of gathering azobenzenes in one molecule and the effect of the cobalt(II) or cobalt(III) ion were investigated using UV–vis absorption spectroscopy, femtosecond transient spectroscopy, and ^1H NMR spectroscopy. In the photostationary state of these four complexes, nearly 50% of the *trans*-azobenzene moieties of the Co(II) complexes were converted to the *cis* isomer, and nearly 10% of the *trans*-azobenzene moieties of the Co(III) complexes isomerized to the *cis* isomer, implying that the *cis* isomer ratio in the photostationary state upon irradiation at 365 nm is controlled not by the number of azobenzene moieties in one molecule but rather by the oxidation state of the cobalt ions. The femtosecond transient absorption spectra of the ligands and the complexes suggested that the photoexcited states of the azobenzene moieties in the Co(III) complexes were strongly deactivated by electron transfer from the azobenzene moiety to the cobalt center to form an azobenzene radical cation and a Co(II) center. The cooperation among the photochemical structural changes of six azobenzene moieties in $[\text{Co}^{\text{II}}(\text{dmAB})_3](\text{BF}_4)_2$ was investigated with ^1H NMR spectroscopy. The time-course change in the ^1H NMR signals of the methyl protons indicated that each azobenzene moiety in $[\text{Co}^{\text{II}}(\text{dmAB})_3](\text{BF}_4)_2$ isomerized to a *cis* isomer with a random probability of 50% and without interactions among the azobenzene moieties.

Introduction

Photochromism is defined as a reversible phototransformation of a chemical species between two forms with different absorption spectra. Photoisomerization causes not only absorption-induced spectral changes but also various changes in physicochemical properties such as the refractive index, the dielectric constant, the redox potential, and the geometrical structure. Photochromic molecules have attracted a significant amount of attention recently because of the possible application of these molecules in the development of various photonic devices, such as erasable optical memory media and optical switch components.¹

Considering the rich variety of properties of certain metal ion complexes (light absorption and emission, energy and electron transfer, etc.), study of the combination of metal ion coordination centers with organic photochromic units has been of interest.² By the fusion of the two independently functional molecular units, many functional molecules can be produced, as in such molecules, isomerization will change the properties of the metal complexes, and the photoisomerization properties will be affected by the metal ion. In fact, previous studies have demonstrated that photochromic molecules attached to metal complexes exhibit unique properties that are not observed in common organic photo-

* To whom correspondence should be addressed. Phone: +81-3-5841-4346. Fax: +81-3-5841-8063. E-mail: nishihara@chem.s.u-tokyo.ac.jp.

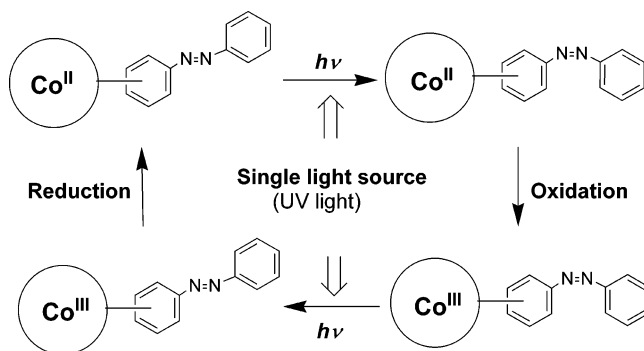
[†] The University of Tokyo.

[‡] Kwansai Gakuin University.

(1) (a) Irie, M. *Chem. Rev.* **2000**, *100*, 1683. (b) Ikeda T.; Tsutsumi, O. *Science* **1995**, *268*, 1873. (c) Kawata S.; Kawata, Y. *Chem. Rev.* **2000**, *100*, 1777.
(2) (a) Nishihara, H. *Bull. Chem. Soc. Jpn.* **2005**, *77*, 407. (b) Nishihara, H. *Coord. Chem. Rev.* **2005**, *249*, 1468.

chromic molecules. A number of studies reported to date have investigated photoswitching of the emission from metal complexes.^{3,4} Photoisomerization is also known to affect the structure of metal complexes.⁵ Some complexes show photochromic behavior due to excitation of a metal-to-ligand charge-transfer band.⁶ We have previously investigated the photochemical properties of azobenzene-bound bipyridine and terpyridine metal complexes.^{4,7–9} Tris(bipyridine)cobalt complexes exhibit a number of interesting behaviors, including (1) a simple electronic structure exhibiting only weak $\pi-\pi^*$ absorption bands in the UV region and very weak $d-d^*$ absorption in the visible region, which could simplify photochemical investigations, and (2) the reversible redox behavior of cobalt bipyridine complexes, which yields electron-related phenomena of interest, including light-induced electron transfer.^{10,11} We have found that the Co(III) complexes $[\text{Co}(\text{pAB})_3](\text{BF}_4)_3$ {pAB = 4-[4-(4-tolylazo)phenyl]-2,2'-bipyridine} and $[\text{Co}(\text{mAB})_3](\text{BF}_4)_3$ {mAB = 4-[3''-(4'''-tolylazo)phenyl]-2,2'-bipyridine} significantly prevent formation of the cis isomer by UV light irradiation, whereas the corresponding Co(II) complexes do not. This result could be applied to realize the reversible trans–cis photoisomerization of azobenzene moieties using a single UV light source and the $\text{Co}^{\text{III}}/\text{Co}^{\text{II}}$ redox reaction (Scheme 1); preliminary results have been reported in previous communications.^{8,9} In the present study, we prepared the six-azobenzene-bound tris(bipyridine)cobalt complexes $[\text{Co}(\text{dmAB})_3](\text{BF}_4)_2$ and $[\text{Co}(\text{dmAB})_3](\text{BF}_4)_3$ {dmAB = 4,4'-bis-[3''-(4'''-tolylazo)phenyl]-2,2'-bipyridine} (see Chart 1) and investigated their photoisomerization behaviors, as well as those of the corresponding mAB complexes. We also carried out transient spectroscopic measurements of the photochemi-

Scheme 1. Reversible Isomerization Using a Single Light Source and Redox Reaction



cal processes regarding interactions between the ligands and their complexes. The process of structural changes in $[\text{Co}(\text{dmAB})_3](\text{BF}_4)_2$ upon photoirradiation was monitored using ^1H NMR spectroscopy to examine the occurrence of intramolecular cooperative motion during azobenzene isomerization. On the basis of these results, the role played by a cobalt center in the photoisomerization reaction of the azobenzene moieties in these complexes was identified.

Results and Discussion

Syntheses. The two-azobenzene-bound ligand, i.e., the dmAB ligand, was prepared via dinitro and diamino compounds, starting with 4,4'-dibromobipyridine¹² (see Scheme S1, Supporting Information). The product of the Suzuki coupling reaction of 4,4'-dibromobipyridine¹³ with 3-nitrophenylboronic acid was purified by filtration from the reaction mixture, affording a white solid of 4,4'-bis(3''-nitrophenyl)-2,2'-bipyridine (**1**). Compound **1** could then be separated from the catalyst and excess boronic acid by washing the reaction mixture with water, toluene, and ether, because of the poor solubility of compound **1**, which is highly air-stable, but is almost insoluble in typical organic solvents such as acetone, chloroform, dichloromethane, and toluene.

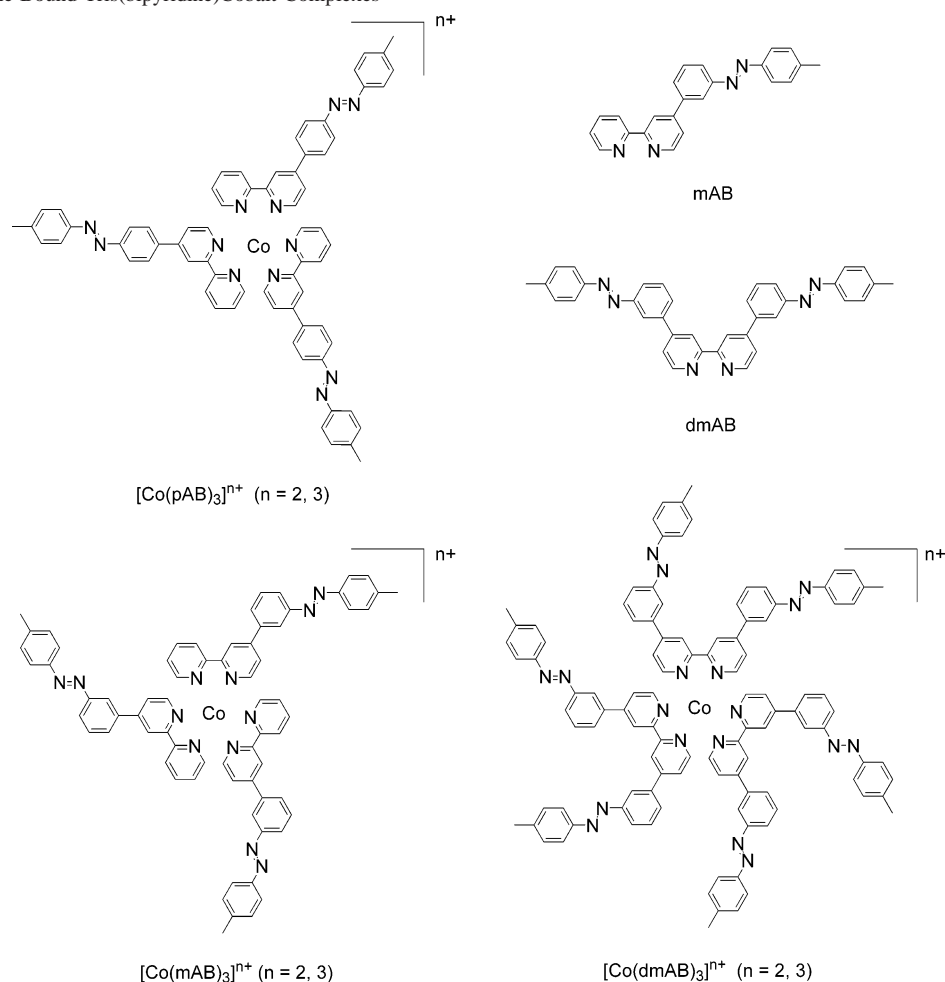
The reduction of the nitro moieties of **1** proceeded with tin(II) chloride under reflux conditions (100 °C).¹⁴ The resulting product, 4,4'-bis(3''-aminophenyl)-2,2'-bipyridine (**2**), was obtained as a white solid that was air-stable and slightly soluble in organic solvents. The azo moieties were formed by the condensation of nitrosotoluene and **2** in fairly good yield. The resulting ligand, dmAB, was air-stable; soluble in acetone, dichloromethane, chloroform, and toluene; and insoluble in methanol, acetonitrile, and *n*-hexane. The structure of dmAB was determined by single-crystal X-ray diffraction analysis (see Table S1 and Figure S1, Supporting Information).

The Co(II) complex $[\text{Co}(\text{dmAB})_3](\text{BF}_4)_2$ was obtained by the reaction of dmAB with cobalt(II) chloride, leading to the formation of $[\text{Co}^{\text{II}}(\text{dmAB})_3]\text{Cl}_2$, which is soluble in

- (3) (a) Norsten, T. B.; Branda, N. R. *Adv. Mater.* **2001**, *13*, 347. (b) Myles, A. J.; Branda, N. R. *Adv. Funct. Mater.* **2002**, *12*, 167. (c) Juke, R. T. F.; Adamo, V.; Hartl, F.; Belsler, P.; De Cola, L. *Inorg. Chem.* **2004**, *43*, 2779. (d) Takayama, K.; Matsuda, K.; Irie, M. *Chem. Eur. J.* **2003**, *9*, 5605. (e) Fernández-Acebes, A.; Lehn, J.-M. *Chem. Eur. J.* **1999**, *5*, 3285.
- (4) Yutaka, T.; Mor, I.; Kurihara, M.; Mizutani, J.; Tamai, N.; Kawai, T.; Irie, M.; Nishihara, H. *Inorg. Chem.* **2002**, *41*, 7143.
- (5) Matsuda, K.; Irie, M. *J. Photochem. Photobiol. C: Photochem. Rev.* **2004**, *5*, 169.
- (6) (a) Yam, V. W.-W.; Yang, Y.; Zhang, J.; Chu, B. W.-K.; Zhu, N. *Organometallics* **2001**, *20*, 4911. (b) Kurihara, M.; Hirooka, A.; Kume, S.; Sugimoto, M.; Nishihara, H. *J. Am. Chem. Soc.* **2002**, *124*, 8800. (c) Nihei, M.; Kurihara, M.; Mizutani, J.; Nishihara, H. *Chem. Lett.* **2001**, 852. (d) Nihei, M.; Kurihara, M.; Mizutani, J.; Nishihara, H. *J. Am. Chem. Soc.* **2003**, *125*, 2964. (e) Sakamoto, R.; Murata, M.; Kume, S.; Sampei, H.; Sugimoto, M.; Nishihara, H. *Chem. Commun.* **2005**, 1215.
- (7) (a) Yutaka, T.; Kurihara, M.; Nishihara, H. *Mol. Cryst. Liq. Cryst.* **2000**, *343*, 511. (b) Yutaka, T.; Kurihara, M.; Kubo, K.; Nishihara, H. *Inorg. Chem.* **2000**, *39*, 3438. (c) Yutaka, T.; Mori, I.; Kurihara, M.; Mizutani, J.; Kubo, K.; Furusho, S.; Matsumura, K.; Tamai, N.; Nishihara, H. *Inorg. Chem.* **2001**, *40*, 4986. (d) Yutaka, T.; Mori, I.; Kurihara, M.; Tamai, N.; Nishihara, H. *Inorg. Chem.* **2003**, *42*, 6306. (e) Kume, S.; Kurihara, M.; Nishihara, H. *Inorg. Chem.* **2003**, *42*, 2194. (f) Kume, S.; Murata, M.; Ozeki, T.; Nishihara, H. *J. Am. Chem. Soc.* **2005**, *127*, 490.
- (8) Kume, S.; Kurihara, M.; Nishihara, H. *J. Chem. Soc., Chem. Commun.* **2001**, 1656.
- (9) Kume, S.; Kurihara, M.; Nishihara, H. *J. Korean Electrochem. Soc.* **2002**, *5*, 189.
- (10) Oregan, B.; Grätzel, M. *Nature* **1991**, *353*, 737.
- (11) (a) Torieda, H.; Nozaki, K.; Yoshimura, A.; Ohno, T. *J. Phys. Chem. A* **2004**, *108*, 4819. (b) Buranda, T.; Lei, Y.; Endicott, J. F. *J. Am. Chem. Soc.* **1992**, *114*, 6916.

- (12) (a) Murase, I. *Nippon Kagaku Zasshi* **1956**, *77*, 682. (b) Haginiwa, J. *Yakugaku Zasshi* **1955**, *75*, 731. (c) Anderson, S.; Constable, E. C.; Seddon, K. R.; Turp, J. E. *J. Chem. Soc., Dalton Trans.* **1985**, 2247. (d) Maerker, G.; Case, F. H. *J. Am. Chem. Soc.* **1958**, *80*, 2475.
- (13) Damrauer, N. H.; Boussie, T. R.; Devenney, M.; McCusker, J. K. *J. Am. Chem. Soc.* **1997**, *119*, 8253.
- (14) Filer, C. N.; Granchelli, F. E.; Soloway, A. H.; Neumeier, J. L. *J. Org. Chem.* **1978**, *43*, 672.

Chart 1. Azobenzene-Bound Tris(bipyridine)Cobalt Complexes



methanol. Because dmAB is insoluble in methanol, $[\text{Co}^{\text{II}}(\text{dmAB})_3]\text{Cl}_2$ could be separated from the ligand dmAB. Then, the anion exchange of Cl^- for BF_4^- gave a pure orange solid of $[\text{Co}(\text{dmAB})_3](\text{BF}_4)_2$. The $\text{Co}(\text{III})$ complex $[\text{Co}(\text{dmAB})_3](\text{BF}_4)_3$ was prepared by the reaction of dmAB with cobalt(II) nitrate, followed by oxidation with Ag^+ . After anion exchange, reprecipitation of the mixture from acetonitrile/diethyl ether and dichloromethane/diethyl ether gave a pure orange solid of $[\text{Co}^{\text{III}}(\text{dmAB})_3](\text{BF}_4)_3$. Both Co dmAB complexes were soluble in chloroform, dichloromethane, and acetonitrile.

For the synthesis of the one-azobenzene-bound ligand, mAB, the starting material 4-(3''-nitrophenyl)-2,2'-bipyridine (3) was prepared from 3-(3'-carboxy-3'-oxo-1'-propenyl)-nitrobenzene.¹⁵ The synthesis from the nitro derivative to mAB and the syntheses of the $\text{Co}(\text{II})$ and $\text{Co}(\text{III})$ complexes of mAB, $[\text{Co}(\text{dmAB})_3](\text{BF}_4)_2$ and $[\text{Co}(\text{dmAB})_3](\text{BF}_4)_3$, respectively, were similar to the methods used for the syntheses of dmAB and its complexes (see Scheme S2, Supporting Information).

UV–Vis Absorption Spectra. UV–vis absorption spectra of the ligands dmAB and mAB and their cobalt(III) and cobalt(II) complexes in dichloromethane are displayed in

Figure 1. Selected spectral data are presented together with those of the related compounds azobenzene and bipyridine in Table 1. The peak absorbance in the dmAB spectrum was almost twice that in the mAB spectrum, except that the $\pi-\pi^*$ transition derived from the bipyridine moiety at ~ 290 nm was similar. A weak $n-\pi^*$ transition of the azo groups, the transition energy of which is known to be less significantly affected by substituents,¹⁶ was observed at 440, 444, and 444 nm in the spectra of azotoluene, dmAB, and mAB, respectively. The $\pi-\pi^*$ bands of the azo group were observed at 336 and 332 nm for dmAB and mAB, respectively, with little shift compared to that of azotoluene (334 nm), which indicated the weak conjugation of the bipyridine moiety with the azo moiety. However, in the case of pAB, in which the π conjugation is extended to the bipyridine moiety, the azo $\pi-\pi^*$ band was observed at a longer wavelength ($\lambda_{\text{max}} = 342$ nm).⁸

The absorption spectra of dmAB, $[\text{Co}^{\text{II}}(\text{dmAB})_3](\text{BF}_4)_2$, and $[\text{Co}^{\text{III}}(\text{dmAB})_3](\text{BF}_4)_3$, are shown in Figure 1A, and the spectra of mAB, $[\text{Co}^{\text{II}}(\text{mAB})_3](\text{BF}_4)_2$, and $[\text{Co}^{\text{III}}(\text{mAB})_3](\text{BF}_4)_3$ are shown in Figure 1B. The intensities of the azo $\pi-\pi^*$ bands of the dmAB complexes were almost twice those of the mAB complexes, as expected from the numbers

(15) (a) Kipp, R. A.; Li, Y.; Simon, J. A.; Schmehl, R. H. *J. Photochem. Photobiol.* **1999**, *121*, 27. (b) Krönke, F. *Synthesis* **1976**, *1*, 1.

(16) Forber, C. L.; Kelusky, E. C.; Bunce, J. B.; Zerner, M. C. *J. Am. Chem. Soc.* **1985**, *107*, 5884.

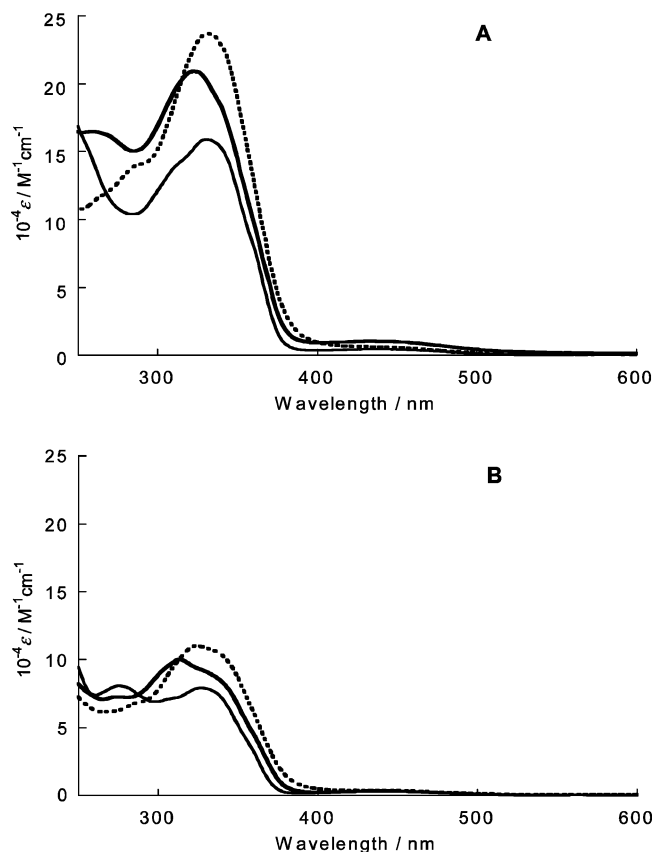


Figure 1. UV–vis absorption spectra of ligands and cobalt complexes: (A) dmAB (thin solid line), $[\text{Co}^{\text{II}}(\text{dmAB})_3](\text{BF}_4)_2$ (solid line), and $[\text{Co}^{\text{III}}(\text{dmAB})_3](\text{BF}_4)_3$ (dotted line); (B) mAB (thin solid line), $[\text{Co}^{\text{II}}(\text{mAB})_3](\text{BF}_4)_2$ (solid line), and $[\text{Co}^{\text{III}}(\text{mAB})_3](\text{BF}_4)_3$ (dotted line). The spectra of the ligands are enlarged three-fold to normalize the number of azo moieties.

Table 1. UV–Vis Absorption Spectral Data

compound	$\lambda_{\text{maz}}/\text{nm}$ ($10^{-4}\epsilon/\text{M}^{-1}\text{cm}^{-1}$)		
	azo $n-\pi^*$	azo $\pi-\pi^*$	bpy $\pi-\pi^*$
bpy			287 (1.4)
azotoluene	440 (0.12)	334 (1.9)	—
dmAB	444 (0.15)	336 (5.2)	—
mAB	444 (0.10)	336 (5.2)	280 (2.7)
pAB	443 (0.16)	342 (3.2)	283 (1.9)
$[\text{Co}^{\text{II}}(\text{dmAB})_3](\text{BF}_4)_2$	434 (1.0)	320 (21)	—
$[\text{Co}^{\text{III}}(\text{dmAB})_3](\text{BF}_4)_3$	sh	328 (24)	—
$[\text{Co}^{\text{II}}(\text{mAB})_3](\text{BF}_4)_2$	434 (0.30) sh	334 (8.3) sh	—
$[\text{Co}^{\text{III}}(\text{mAB})_3](\text{BF}_4)_3$	434 (0.4) sh	337 (10) sh	—
$[\text{Co}^{\text{II}}(\text{pAB})_3](\text{BF}_4)_2$	sh	360 (11)	—
$[\text{Co}^{\text{III}}(\text{pAB})_3](\text{BF}_4)_3$	sh	375 (9.7)	—

of azobenzene moieties in the molecules. The maximum wavelength of the azo $\pi-\pi^*$ band differed slightly between $[\text{Co}^{\text{II}}(\text{dmAB})_3](\text{BF}_4)_2$ and $[\text{Co}^{\text{III}}(\text{dmAB})_3](\text{BF}_4)_3$, as well as between $[\text{Co}^{\text{II}}(\text{mAB})_3](\text{BF}_4)_2$ and $[\text{Co}^{\text{III}}(\text{mAB})_3](\text{BF}_4)_3$, and these differences were substantially smaller than those in the case of $[\text{Co}^{\text{II}}(\text{pAB})_3](\text{BF}_4)_2$ and $[\text{Co}^{\text{III}}(\text{pAB})_3](\text{BF}_4)_3$ (Table 1), indicating weaker interactions between the azobenzene moieties and $[\text{Co}(\text{bpy})_3]^{n+}$ ($n = 2, 3$).

Redox Properties and Spin States of the Complexes. It is known that tris(bipyridine)cobalt undergoes two-step one-electron reversible redox reactions of $\text{Co}^{\text{III}}/\text{Co}^{\text{II}}$ and $\text{Co}^{\text{II}}/\text{Co}^{\text{I}}$ couples¹⁷ and that azobenzene is reduced to give an azoben-

Table 2. Redox Properties^a

compound	$\text{Co}^{\text{III}}/\text{Co}^{\text{II}}$		$\text{Co}^{\text{II}}/\text{Co}^{\text{I}}$		azo ⁰ /azo ⁻	
	E°/V	$\Delta E_p/\text{mV}$	E°/V	$\Delta E_p/\text{mV}$	E°/V	$\Delta E_p/\text{mV}$
azotoluene ^b	—	—	—	—	-1.99	88
$[\text{Co}^{\text{III}}(\text{dmAB})_3](\text{BF}_4)_3$	-0.04	84	-1.16	71	-1.83	155
$[\text{Co}^{\text{III}}(\text{mAB})_3](\text{BF}_4)_3$	-0.15	84	-1.27	69	-1.82	111
$[\text{Co}^{\text{III}}(\text{pAB})_3](\text{BF}_4)_3$ ^b	-0.15	59	-1.28	89	-1.72	102

^a E° values were estimated from the anodic and cathodic peak potentials, $(E_{p,a} + E_{p,c})/2$, in the cyclic voltammogram obtained at a scan rate of 0.1 V/s in 0.1 M $\text{Bu}_4\text{NBF}_4/\text{CH}_2\text{Cl}_2$ and referred to Fc^+/Fc unless otherwise stated. $\Delta E_p = E_{p,a} + E_{p,c}$. ^b In 0.1 M $\text{Bu}_4\text{NBF}_4/\text{MeCN}$.

zene anion radical.¹⁸ The azobenzene-attached complexes $[\text{Co}^{\text{III}}(\text{dmAB})_3](\text{BF}_4)_3$, $[\text{Co}^{\text{III}}(\text{mAB})_3](\text{BF}_4)_3$, and $[\text{Co}^{\text{III}}(\text{mAB})_3](\text{BF}_4)_3$ exhibit two reversible redox reactions of $\text{Co}^{\text{III}}/\text{Co}^{\text{II}}$ and $\text{Co}^{\text{II}}/\text{Co}^{\text{I}}$ couples and further quasireversible reduction of the azobenzene moieties (see Figure S4, Supporting Information). Redox potentials are summarized in Table 2. The E° values of the $\text{Co}^{\text{III}}/\text{Co}^{\text{II}}$ and $\text{Co}^{\text{II}}/\text{Co}^{\text{I}}$ couples are shifted for the dmAB complex compared to those of the mAB and pAB complexes by the stronger electron-withdrawing effect of six azobenzene groups. In the cyclic voltammetry of $[\text{Co}^{\text{III}}(\text{mAB})_3](\text{BF}_4)_3$ and $[\text{Co}^{\text{III}}(\text{mAB})_3](\text{BF}_4)_3$ in 0.1 M $\text{Bu}_4\text{NBF}_4/\text{MeCN}$, reduction of the bipyridine moieties occurred at more negative potential than reduction of the azobenzene moieties, giving multiple waves in the potential region between -1.3 and 2.5 V vs ferrocenium/ferrocene (Fc^+/Fc).

$[\text{Co}^{\text{II}}(\text{bpy})_3]^{2+}$ is generally known to be a typical high-spin d^7 complex.¹⁹ When Co(II) is in the high-spin d^7 ($t_{2g}^5e_g^2$) configuration, the complex will have an undistorted complete octahedral structure. In contrast, low-spin d^7 ($t_{2g}^6e_g^1$) Co(II) complexes are often found in a highly Jahn–Teller-distorted octahedral structure. Initially, we expected that the coordination environment of $[\text{Co}^{\text{II}}(\text{dmAB})_3](\text{BF}_4)_2$ would be complex because of the existence of six bulky and electron-withdrawing azobenzene moieties, so that the Jahn–Teller distortion effect might appear;²⁰ the magnetic susceptibility of $[\text{Co}^{\text{II}}(\text{dmAB})_3](\text{BF}_4)_2$ was thus measured. The χT value was found to be almost independent of the temperature (50, 100, 200, and 300 K) and was 2 emu K mol^{-1} , which is similar to the theoretical value of the typical Co(II) high-spin state of the d^7 ($t_{2g}^5e_g^2$) configuration ($S = 3/2$) (assuming that $g = 2$, the theoretical χT value is 1.875 emu K mol^{-1}), and is similar to the χT value of $[\text{Co}^{\text{II}}(\text{bpy})_3]^{2+}$ (see Table S2, Supporting Information).

The results discussed above indicate that the bulky azobenzene moieties do not affect either the structure of the complex or the spin state of the Co(II) ion. Therefore, the six azobenzene moieties can be assumed to be located at almost equal distances from the cobalt ion. This is significant information for the investigation of the photoisomerization of the six azobenzene moieties in $[\text{Co}^{\text{II}}(\text{dmAB})_3](\text{BF}_4)_2$ (vide infra).

(18) Bard, A. J.; Faulkner, L. R. *Electrochemical Methods—Fundamentals and Applications*; Wiley: New York, 1980.

(19) Hauser, A.; Amstutz, N.; Deahay, S.; Sadki, A.; Schenker, S.; Sieber, R.; Zerara, M. *Struct. Bonding* **2004**, 106, 81.

(20) Beattie, J. K.; Elsbernd, H. *Inorg. Chim. Acta* **1995**, 240, 641.

(17) (a) Vydra, F.; Pribil, R. *Talanta* **1961**, 8, 824. (b) Tanaka, N.; Sato, Y. *Bull. Chem. Soc. Jpn.* **1968**, 41, 2059.

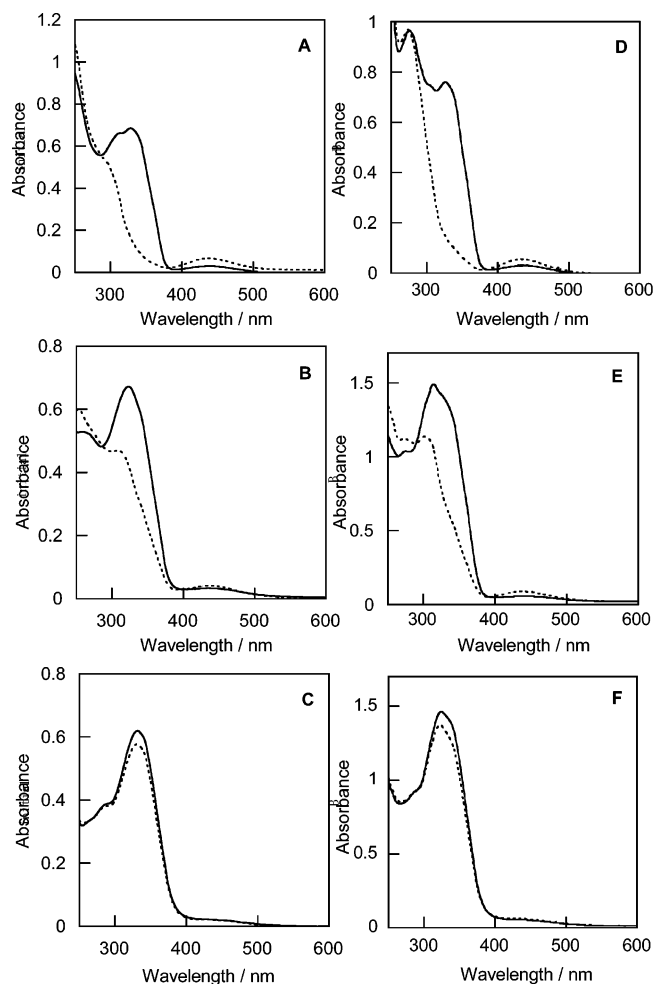


Figure 2. UV-vis spectral changes of (A) dmAB, (B) $[\text{Co}^{\text{II}}(\text{dmAB})_3]^{2+}$, (C) $[\text{Co}^{\text{II}}(\text{dmAB})_3]^{3+}$, (D) mAB, (E) $[\text{Co}^{\text{II}}(\text{mAB})_3]^{2+}$, and (F) $[\text{Co}^{\text{II}}(\text{mAB})_3]^{3+}$ in dichloromethane upon irradiation with 365-nm light from the initial spectra (solid line) to the spectra in the PSS (dotted line).

Photoisomerization Behavior of dmAB and mAB Complexes. Figure 2 shows the absorption spectral changes of dmAB, $[\text{Co}^{\text{II}}(\text{dmAB})_3]^{2+}$, and $[\text{Co}^{\text{III}}(\text{dmAB})_3]^{3+}$ upon UV irradiation at 365 nm in dichloromethane. In the case of dmAB, the azo $\pi-\pi^*$ band at 330 nm decreased, and the azo $n-\pi^*$ band at 431 nm increased in intensity; moreover, the spectrum was reversed to the initial state by visible-light irradiation at 436 nm. These spectral changes are suggestive of the typical trans-to-cis isomerization of azobenzene moieties. Trans-to-cis conversion proceeded almost completely, as the ^1H NMR spectral changes of dmAB in dichloromethane- d_2 upon UV irradiation suggest that 97% of the *trans*-azobenzene moieties converted to the cis isomer when in the photostationary state (PSS). In the spectrum of $[\text{Co}^{\text{II}}(\text{dmAB})_3]^{2+}$, a decrease in the azo $\pi-\pi^*$ band and an increase in the azo $n-\pi^*$ band were observed upon irradiation at 365 nm, and the spectral changes were reversed by irradiation at 436 nm. On the other hand, slight absorbance changes were observed in the spectrum of $[\text{Co}^{\text{III}}(\text{dmAB})_3]^{3+}$ upon UV irradiation. The ratio of the newly formed cis isomer in the PSS, estimated from the decrease in the azo $\pi-\pi^*$ band, was 51% for $[\text{Co}^{\text{II}}(\text{dmAB})_3]^{2+}$ (at 354 nm) and 9% for $[\text{Co}^{\text{III}}(\text{dmAB})_3]^{3+}$ (at 360 nm). Steric interactions

Table 3. Ratio of the Cis Isomer in the PSS (%)

compound	from UV-vis spectroscopy	from ^1H NMR spectroscopy
dmAB	<i>a</i>	97
$[\text{Co}^{\text{II}}(\text{dmAB})_3](\text{BF}_4)_2$	51	53
$[\text{Co}^{\text{III}}(\text{dmAB})_3](\text{BF}_4)_3$	9	7
mAB	<i>a</i>	94
$[\text{Co}^{\text{II}}(\text{mAB})_3](\text{BF}_4)_2$	57	<i>a</i>
$[\text{Co}^{\text{III}}(\text{mAB})_3](\text{BF}_4)_3$	9	<i>a</i>

^a Not determined.

among the six azo moieties appear to have been unlikely, because the 4 position is too far to allow an interaction in the $[\text{Co}^{\text{II}}(\text{bpy})_3]^{2+}$ cation.²¹ The electronic interactions among the azo moieties thus appear to be weak, as the spectral change has an isosbestic point, implying that the first trans-to-cis isomerization exerts no electronic effect on the other five *trans*-azo moieties in the same complex; moreover, the subsequent isomerization occurs in the same manner as the first isomerization (vide infra). The mAB compounds underwent a photoisomerization reaction upon exposure to 365-nm UV light, which is similar to the effect on dmAB compounds, and the cis ratio in the PSS was 94% for free mAB (estimated from the ^1H NMR spectral changes), 57% for $[\text{Co}^{\text{II}}(\text{mAB})_3](\text{BF}_4)_2$, and 9% for $[\text{Co}^{\text{III}}(\text{mAB})_3](\text{BF}_4)_3$ (estimated from the UV spectral changes) in dichloromethane.

The trans-to-cis ratios of the dmAB compounds and mAB compounds are summarized in Table 3. In regions of $[\text{Co}^{\text{II}}(\text{dmAB})_3](\text{BF}_4)_2$ and $[\text{Co}^{\text{III}}(\text{dmAB})_3](\text{BF}_4)_3$, the ratio of the cis isomer, as estimated from the absorption spectra, was compared with that estimated from ^1H NMR spectral changes. The photoisomerization behavior of $[\text{Co}^{\text{II}}(\text{dmAB})_3](\text{BF}_4)_2$ and $[\text{Co}^{\text{III}}(\text{dmAB})_3](\text{BF}_4)_3$ could be observed in the ^1H NMR spectra, despite the paramagnetic nature of the $[\text{Co}^{\text{II}}(\text{bpy})_3]^{2+}$ moiety, because the electron of the cobalt(II) center appears to affect only the coordinated N atoms and the neighboring C atoms on the bipyridine moieties (vide infra). The ratios of the cis isomer estimated from the absorption spectral changes were in reasonable agreement with those estimated from the ^1H NMR spectral changes, indicating that the intensity of the absorption band of the $\pi-\pi^*$ transition of the *cis*-azobenzene moieties was substantially lower than that of the *trans*-azobenzene moieties. When the ligands and cobalt(III/II) complexes in the dmAB compounds and mAB compounds were compared, the ligands were found to isomerize almost entirely to the cis isomer. In contrast, the cobalt complexes exhibited only incomplete photoisomerization behavior, depending on the oxidation state of the cobalt center.

The redox-dependent photoisomerization phenomenon is apparently governed by the interaction between the azobenzene moieties and the $[\text{Co}(\text{bpy})_3]^{n+}$ ($n = 2, 3$) moieties; the $[\text{Co}^{\text{III}}(\text{bpy})_3]^{3+}$ moiety exerts a strong suppressing effect on trans-to-cis photoisomerization, whereas the $[\text{Co}^{\text{II}}(\text{bpy})_3]^{2+}$ moiety has a weaker effect. There are some rational accounts

(21) Szalda, D. J.; Creutz, C.; Mahajan, D.; Sutin, N. *Inorg. Chem.* **1983**, *22*, 2372.

of this photoisomerization behavior, depending on the oxidation state of cobalt, as follows:

(1) The difference between electron-withdrawing effects in $[\text{Co}^{\text{III}}(\text{bpy})_3]^{3+}$ and $[\text{Co}^{\text{II}}(\text{bpy})_3]^{2+}$ might lead to a change in the dipole moment around the azo moiety that results in a change in the cis yield in the PSS.

(2) The difference between the absorption spectra of Co(II) complexes and Co(III) complexes might also provide an explanation. The absorbance of the mAB and dmAB complexes at 365 nm is composed of an azo $\pi-\pi^*$ band and weak $\pi-\pi^*$ bands of $[\text{Co}^{\text{II}}(\text{bpy})_3]^{2+}$ or $[\text{Co}^{\text{III}}(\text{bpy})_3]^{3+}$ (vide supra).²² The photoirradiation at 365 nm apparently leads to trans-to-cis photoisomerization of the azobenzene moieties, whereas it might possibly excite the weak $\pi-\pi^*$ band of $[\text{Co}^{\text{II}}(\text{bpy})_3]^{2+}$ or $[\text{Co}^{\text{III}}(\text{bpy})_3]^{3+}$, which might, in turn, be followed by energy transfer to the azo $n-\pi^*$ band and cis-to-trans photoisomerization.

(3) The electronic interaction between the π and/or π^* orbital of the azo moiety and the cobalt d orbital in the photoexcited states, which causes electron transfer or energy transfer, might occur from the excited azo moiety to the cobalt center, and the trans-to-cis isomerization of azobenzene moieties might, in turn, be suppressed.

Comparison of the cis ratios between the dmAB series and the mAB series provides relevant information regarding an interpretation of the results. It should be noted that the yield of the cis isomer in the case of $[\text{Co}^{\text{III}}(\text{dmAB})_3](\text{BF}_4)_3$, 51%, was almost the same as that for $[\text{Co}^{\text{III}}(\text{mAB})_3](\text{BF}_4)_3$, 57%, and the cis isomer yield in $[\text{Co}^{\text{II}}(\text{dmAB})_3](\text{BF}_4)_3$, 9%, was the same as that for $[\text{Co}^{\text{II}}(\text{mAB})_3](\text{BF}_4)_3$. These findings cannot be explained by the first rationale, i.e., the difference between the electron-withdrawing effects in $[\text{Co}^{\text{III}}(\text{bpy})_3]^{3+}$ and $[\text{Co}^{\text{II}}(\text{bpy})_3]^{2+}$, which would lead to a weaker suppression of cis formation among the dmAB complexes composed of six azobenzene moieties than among the mAB complexes composed of three azobenzene moieties; hence, the azobenzene moieties in the dmAB complexes would be expected to give a higher cis yield than those of the mAB complexes. The second rationale, i.e., the difference between the molar absorption coefficients of $[\text{Co}^{\text{II}}(\text{bpy})_3]^{2+}$ and $[\text{Co}^{\text{III}}(\text{bpy})_3]^{3+}$, might lead to a change in the rate of trans-to-cis or cis-to-trans photoisomerization. Thus, the cis yield should be higher in the case of $[\text{Co}^{\text{III}}(\text{dmAB})_3](\text{BF}_4)_3$ with six azobenzene moieties than in the case of $[\text{Co}^{\text{III}}(\text{dmAB})_3](\text{BF}_4)_3$ with three azobenzene moieties, which is not consistent with the results. In the case of the third rationale, i.e., regarding the cause of intramolecular electron transfer or energy transfer, the cis yield would be expected to be independent of the number of azobenzene moieties on a cobalt center, provided that the intensity of the light source was not too high and the relaxation process occurred before the subsequent photon absorption. The effect of the cobalt ion on the photoisomerization behavior was further investigated with femtosecond transient absorption spectroscopy, which enabled us to directly observe the photoexcited-state dynamics (vide infra).²³

(22) Hidaka, J.; Douglas, B. E. *Inorg. Chem.* **1964**, *3*, 1181.

Time-Resolved Transient Absorption Spectra. Figure 3 shows the transient absorption spectra of (A) dmAB and (D) mAB under the $\pi-\pi^*$ (S_2) excitation condition. In these ligands, the spectra obtained just after excitation exhibited a much broader absorption band in the longer-wavelength region (~ 490 nm), and the signal decayed within 1 ps. This band was ascribed to the $S_n \leftarrow S_2$ absorption of the *trans*-azobenzene moieties of dmAB and mAB. The disappearance of the $S_n \leftarrow S_2$ absorption bands was followed by the appearance of an intense absorption band at ~ 420 nm that decayed within 50 ps. This band could be attributed to the $S_n \leftarrow S_1$ absorption of the *trans*-azobenzene moieties of dmAB and mAB. This behavior is very similar to that of the organic azobenzenes reported to date.^{24,25}

Figure 3 also shows the transient absorption spectra under the $\pi-\pi^*$ (S_2) excitation condition of Co(II) and Co(III) complexes of dmAB and mAB. In $[\text{Co}^{\text{II}}(\text{dmAB})_3](\text{BF}_4)_2$ and $[\text{Co}^{\text{II}}(\text{mAB})_3](\text{BF}_4)_2$, the transient spectra progressed in essentially the same manner as did those of the free ligands. On the other hand, a different spectral progression was observed in the cases of $[\text{Co}^{\text{III}}(\text{dmAB})_3]^{3+}$ and $[\text{Co}^{\text{III}}(\text{mAB})_3]^{3+}$. Following the appearance of a broad $S_n \leftarrow S_2$ absorption band, two absorption bands at 410 and 580 nm were observed in both Co(III) complexes, the lifetime of which was extremely long, ca. 10^2 – 10^3 ps. This spectral progression was clearly different from those of the free ligands and the Co(II) complexes. This relaxation process of the Co(III) complexes can be explained by the existence of an electron- or energy-transfer pathway from the photoexcited state of the azobenzene moiety to the Co(III) center. The electron-transfer pathway, which forms an azobenzene radical cation and a Co(II) center, is a likely explanation for the results, as it is energetically possible; the azo π^* level is -1.93 V, and the Co e_g^* level is -0.20 V vs Fc^+/Fc . In addition, it has been reported by Daasbjerg and Sehested that the azobenzene radical cation formed by flash radiolysis exhibits a similar peak around 580 nm.²⁶ The energy-transfer pathway is also possible because the $e_g^* - t_{2g}$ energy difference of the Co(III) center is estimated at 2.75 eV from $\lambda_{\text{maz,d-d}} = 450$ nm, and this energy is smaller than the $\pi-\pi^*$ band energy (3.74 eV) or the $n-\pi^*$ band energy (2.88 eV) of the azobenzene moiety. In this case, excited $\text{Co}^{\text{III}}(\text{bpy})_3$ should be generated, but it was reported that photoexcited $\text{Co}^{\text{III}}(\text{bpy})_3$ did not show any absorption in 550–800-nm region.²⁷ Therefore, it can be concluded that transient absorption spectra with the appearance of the band at 580 nm indicate that the electron-transfer pathway is the main process, although a contribution of energy-transfer process cannot be categorically denied.

(23) (a) Lednev, I. K.; Ye, T.-Q.; Matousek, P.; Towrie, M.; Fogg, P.; Neuwahl, F. V. R.; Umpathy, S.; Hester, R. E.; Moore, J. N. *Chem. Phys. Lett.* **1998**, *290*, 68. (b) Nägele, T.; Hoche, R.; Zinth, W.; Wachtveitl, J. *Chem. Phys. Lett.* **1997**, *272*, 489.

(24) (a) Fujino, T.; Arzhantsev, S. Y.; Tahara, T. *Bull. Chem. Soc. Jpn.* **2002**, *71*, 1031. (b) Azuma, J.; Tamai, N.; Shishido, A.; Ikeda, T. *Chem. Phys. Lett.* **1998**, *288*, 77.

(25) Tamai, N.; Miyasaka, H. *Chem. Rev.* **2000**, *100*, 1875.

(26) (a) Daasbjerg, K.; Sehested, K. *J. Phys. Chem. A* **2003**, *107*, 4462.

(b) Daasbjerg, K.; Sehested, K. *J. Phys. Chem. A* **2002**, *106*, 11098.

(27) Berkoff, R.; Krist, K.; Gafney, H. D. *Inorg. Chem.* **1980**, *19*, 1.

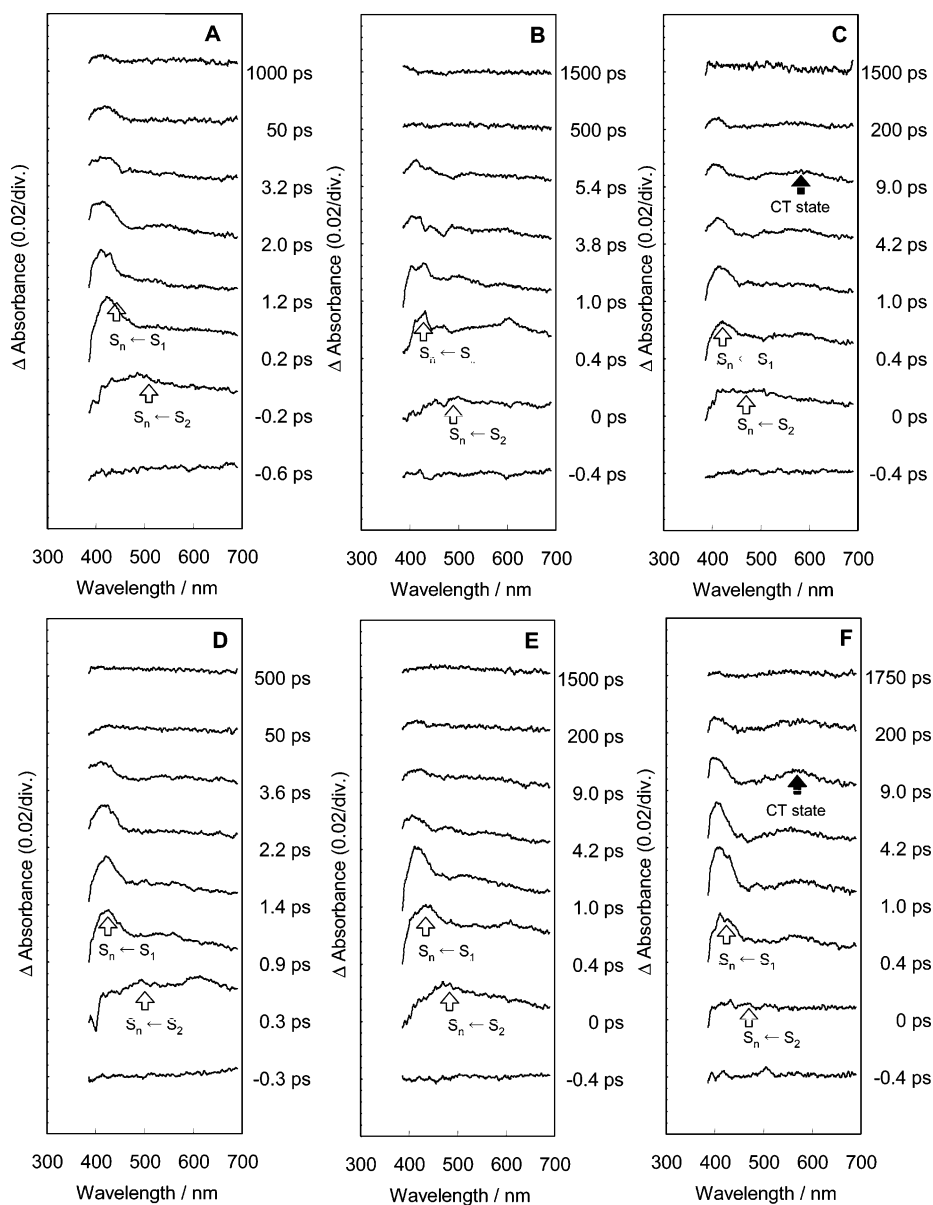


Figure 3. Time-resolved transient absorption spectra of (A) dmAB, (B) $[\text{Co}(\text{dmAB})_3]^{2+}$, (C) $[\text{Co}(\text{dmAB})_3]^{3+}$, (D) mAB, (E) $[\text{Co}(\text{mAB})_3]^{2+}$, and (F) $[\text{Co}(\text{mAB})_3]^{3+}$ in dichloromethane. A 360-nm pulse laser was used for excitation.

Figure 4 shows a schematic representation of the relaxation process and the isomerization paths of the free ligands, Co(II) complexes, and Co(III) complexes. The process of the relaxation of the free ligands and the Co(II) complexes was found to be similar to those of organic azobenzenes. When the *trans*-azobenzene moiety of the Co(III) complexes is excited to the $\pi-\pi^*$ (S_2) state, deactivation of the $\pi-\pi^*$ state occurs, yielding the $n-\pi^*$ (S_1) state, and then the azo⁺-Co(II) charge-transfer state is formed by electron transfer from the azo moiety to the cobalt center. Therefore, the *trans*-to-*cis* photoisomerization pathway in the S_1 excited state is thought to be strongly inhibited by the transition to this charge-separated state.

It should be noted that the average interval of the incident photons is ca. 1 ms, which is substantially longer than the lifetime of the excited state of $[\text{Co}^{\text{III}}(\text{dmAB})_3](\text{BF}_4)_3$ (ca. 1 ns), taking into consideration the intensity of the light source used for the present experiments. Thus, it remains unlikely

that two or more azobenzene moieties are excited simultaneously in both $[\text{Co}^{\text{III}}(\text{dmAB})_3](\text{BF}_4)_3$ and $[\text{Co}^{\text{III}}(\text{mAB})_3](\text{BF}_4)_3$; consequently, it is reasonable to conclude that the same process of inhibition takes place in both complexes.

NMR Observation of the Photoisomerization of Six Azobenzene Moieties in One Molecule. In the ^1H NMR spectra of mAB in dichloromethane- d_2 upon UV-irradiation, the signals of the *trans* isomer were decreased in intensity by 365-nm irradiation, and new signals ascribable to the *cis* isomer appeared at higher magnetic fields (Figure S4, Supporting Information). For the methyl protons, the signal of the *trans* isomer at δ 2.46 ppm decreased in intensity with irradiation at 365 nm, and a new signal ascribable to the *cis* isomer appeared at higher magnetic field (δ 2.29 ppm) (Figure S5, Supporting Information). The shift to the higher magnetic field was caused by the ring current effect, according to the facial structure of the two phenyl rings of an azobenzene moiety in the *cis* form. The integration ratio

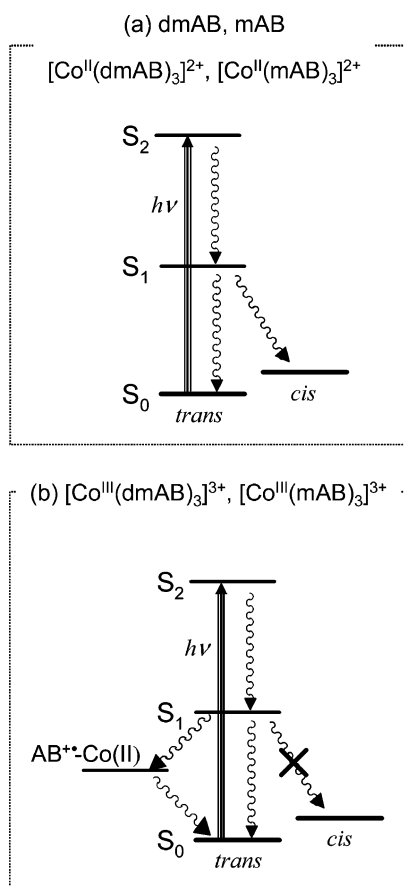


Figure 4. Schematic representation of the relaxation process and isomerization pathways for free ligands and (a) Co(II) complexes and (b) Co(III) complexes.

of the signals for trans and cis isomers indicated that 94% of the trans isomer was converted to the cis isomer by photoirradiation at 365 nm in the PSS.

In this context, there are two possible means of achieving the photoisomerization of the two azobenzene moieties of dmAB: (a) The two azobenzene moieties might isomerize to the cis form simultaneously, or (b) they might isomerize to the cis form in a stepwise manner. Figure 5 shows the ^1H NMR spectral changes of dmAB in dichloromethane- d_2 upon UV irradiation, which indicates the stepwise photoisomerization of dmAB. The signal of the methyl protons of the trans isomer at δ 2.46 ppm decreased in intensity upon irradiation at 365 nm, and two signals ascribable to the cis isomer appeared at higher magnetic field (δ 2.30 and 2.29 ppm). Upon further irradiation at 365 nm, the signal at δ 2.30 ppm decreased, and the signal at δ 2.29 ppm increased in intensity. Thus, the signal at δ 2.30 ppm was ascribed to the methyl protons of the cis-azobenzene moiety of $trans_1,cis_1$ -dmAB, and the signal at δ 2.29 was ascribed to the methyl protons of the cis-azobenzene moieties of cis_2 -dmAB (Figure 5, right). The integration ratio of the signals for the trans and cis isomers indicated that 97% of the trans isomer converted to the cis isomer upon photoirradiation at 365 nm in the PSS. Among the three species ($trans_2$ -dmAB, $trans_1,cis_1$ -dmAB, and cis_2 -dmAB; see Figure 5, right), cis_2 -dmAB was found to be the major species in the PSS.

The photoisomerization of $[\text{Co}(\text{dmAB})_3]^{n+}$ ($n = 2, 3$) complexes, which have six azobenzene moieties in one molecule, could also be observed in the ^1H NMR spectra, despite the presence of the paramagnetic $[\text{Co}^{\text{II}}(\text{bpy})_3]^{2+}$ moiety. In the spectrum of diamagnetic $[\text{Co}^{\text{III}}(\text{dmAB})_3](\text{BF}_4)_3$ in dichloromethane- d_2 , all of the proton signals were observed within the range of δ 2–10 ppm, and these signals were identified using COSY measurements (Figure S6, Supporting Information). In the spectra of paramagnetic $[\text{Co}^{\text{II}}(\text{dmAB})_3](\text{BF}_4)_2$ in dichloromethane- d_2 , the signals of the phenyl rings and methyl groups of $[\text{Co}^{\text{II}}(\text{dmAB})_3]^{2+}$ were observed within the range of δ 2–12 ppm, despite the existence of the paramagnetic $[\text{Co}^{\text{II}}(\text{bpy})_3]^{2+}$ moiety (high-spin d^7), and these signals were identified by COSY measurements (Figure S7, Supporting Information). These findings can be explained by taking into account the facts that azobenzene moieties have weak electronic interactions with $[\text{Co}^{\text{II}}(\text{bpy})_3]^{2+}$ moieties (as azobenzene moieties are meta-substituted to bipyridine) and the rate of the electron self-exchange reaction of $[\text{Co}(\text{bpy})_3]^{3+/2+}$ is very slow, because of the nonadiabaticity resulting from the large spin changes involved²⁸ {the respective ground states of $[\text{Co}^{\text{III}}(\text{bpy})_3]^{3+}$ and $[\text{Co}^{\text{II}}(\text{bpy})_3]^{2+}$ are a singlet and a quartet, respectively}. The signals of the pyridine rings were observed with a paramagnetic shift to approximately δ 40–100 ppm.

In the ^1H NMR spectral changes of $[\text{Co}^{\text{III}}(\text{dmAB})_3](\text{BF}_4)_3$ upon UV irradiation, the signal of the methyl protons of the trans isomer at δ 2.43 ppm decreased slightly, and a new signal ascribable to the cis isomer appeared at δ 2.19 ppm (Figure S8, Supporting Information). The integration ratio of the signals for the trans and cis isomers indicated that 7% of the trans isomer was converted to the cis isomer in the PSS. Taking these results into consideration, the new signal at δ 2.19 ppm was ascribed to the methyl protons of the cis-azobenzene moiety in $trans_1,cis_1$ -dmAB. No signals of the cis-azobenzene moieties of cis_2 -dmAB were observed, indicating that the yield of cis_2 -dmAB was quite low.

Figure 6 shows the ^1H NMR spectral changes in $[\text{Co}^{\text{II}}(\text{dmAB})_3](\text{BF}_4)_2$ upon UV irradiation. The signal of the methyl protons of the trans isomer at δ 2.63 ppm decreased in intensity, and a new signal ascribable to the cis isomer appeared at δ 2.46 ppm upon irradiation at 365 nm. Further irradiation yielded a signal at δ 2.39 ppm. The signal at δ 2.46 ppm that had appeared initially was ascribed to the cis-azobenzene moiety of $trans_1,cis_1$ -dmAB, and the signal at δ 2.39 ppm that appeared after the former signal was ascribed to the cis-azobenzene moieties of cis_2 -dmAB. In the PSS, the integration ratio of the signals at δ 2.63, 2.46, and 2.38 ppm was 2:1:1. The trans-to-cis conversion ratio was found to be 53%, which was almost the same as the value estimated from the absorption spectral changes.

Several conceivable scenarios of cooperation of the six azobenzene moieties in the photoisomerization process can be suggested, all of which would afford a 1:1 trans-to-cis

(28) (a) Jolley, W. H.; Stranks, D. R.; Swaddle, T. W. *Inorg. Chem.* **1990**, *29*, 385. (b) Grace, M. R.; Swaddle, T. W. *Inorg. Chem.* **1993**, *32*, 5597. (c) Beattie, J. K.; Elsebernd, H. *Inorg. Chim. Acta* **1995**, *240*, 641

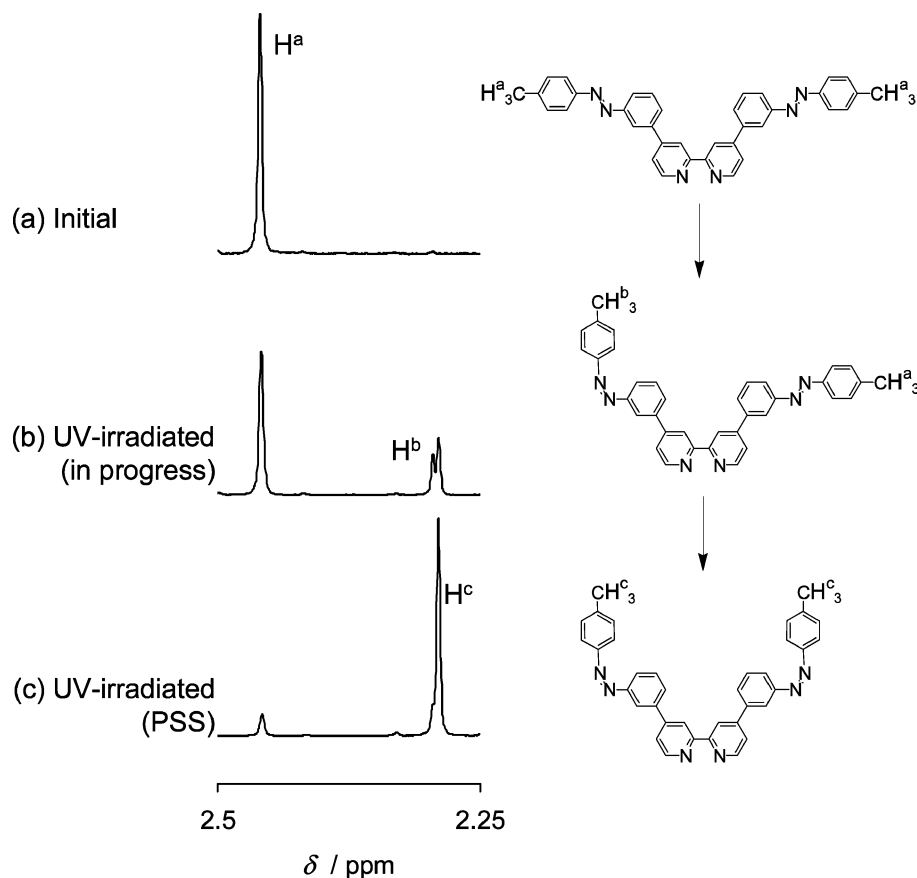


Figure 5. (left) ^1H NMR spectral changes of dmAB upon UV irradiation in CD_2Cl_2 (500 MHz) and (right) a schematic representation of the stepwise photoisomerization, with the assignment of the methyl protons.

Table 4. Ratios of *trans*- and *cis*-Azobenzene Moieties in Cases 1–4

case	<i>trans</i> -AB	<i>cis</i> -AB in <i>trans</i> ₁ , <i>cis</i> ₁ -dmAB	<i>cis</i> -AB in <i>cis</i> ₂ -dmAB
1	1	0	1
2	1	1	0
3	3	1	2
4	2	1	1

ratio in the PSS, as shown in Figure 7. In the first scenario, case 1, the composition would be 50% $[\text{Co}^{\text{II}}(\text{trans}_2\text{-dmAB})_3](\text{BF}_4)_2$ and 50% $[\text{Co}^{\text{II}}(\text{cis}_2\text{-dmAB})_3](\text{BF}_4)_2$. In case 2, the composition would be 100% $[\text{Co}^{\text{II}}(\text{trans}_1, \text{cis}_1\text{-dmAB})_3](\text{BF}_4)_2$. In case 3, the composition would be 100% $[\text{Co}^{\text{II}}(\text{trans}_2\text{-dmAB})(\text{trans}_1, \text{cis}_1\text{-dmAB})(\text{cis}_2\text{-dmAB})](\text{BF}_4)_2$. In case 4, each azobenzene moiety would isomerize to the *cis* form independently with a probability of 50%.

In the case representing the actual situation, the ratio of the three types of azobenzene moiety (i.e., 1, *trans*-azobenzene moieties of *trans*₂-dmAB and *trans*₁,*cis*₁-dmAB; 2, *cis*-azobenzene moieties of *trans*₁,*cis*₁-dmAB; and 3, *cis*-azobenzene moieties of *cis*₂-dmAB) would agree with the integration ratio of the proton signals at δ 2.63, 2.46, and 2.38 ppm. Table 4 shows the ratios of the three types of azobenzene moiety. The ratios in cases 1–3 were found to disagree with those based on the ^1H NMR signals. In case 4, which accounts for $2^6 = 64$ cases, $64 \times 6 = 384$ azobenzene moieties are possible. The ratio of the three types of azobenzene moiety is $192:96:96 = 2:1:1$, which is consistent with the ratio obtained from the ^1H NMR signals.

These results indicate that each azobenzene moiety in $[\text{Co}^{\text{II}}(\text{dmAB})_3](\text{BF}_4)_2$ isomerizes with a random probability of 50%. This interpretation of the results implies that the preceding *trans*-to-*cis* isomerization seems to have no electronic effects on the remaining azobenzene moieties and the subsequent isomerization occurs in the same manner as the preceding isomerization.

Conclusions

This study of the photoisomerization behavior of tris-(bipyridine)cobalt complexes containing six azobenzene moieties, $[\text{Co}^{\text{II}}(\text{dmAB})_3](\text{BF}_4)_2$ and $[\text{Co}^{\text{III}}(\text{dmAB})_3](\text{BF}_4)_3$, and those containing three azobenzene moieties $[\text{Co}^{\text{II}}(\text{mAB})_3](\text{BF}_4)_2$ and $[\text{Co}^{\text{III}}(\text{mAB})_3](\text{BF}_4)_3$ revealed that nearly 50% of the *trans*-azobenzene moieties of the Co(II) complexes were converted to the *cis* isomer and nearly 10% of the *trans*-azobenzene moieties of the Co(III) complexes isomerized to the *cis* isomer in the PSS. This implies that the yield of the *cis* isomer depends on the oxidation state of the cobalt ions, but not on the number of azobenzene moieties in one molecule. Significant hindrance of photoisomerization in the Co(III) complexes appears to take place as a result of the electron transfer from the photoexcited azobenzene moiety to the cobalt center, thus forming an azobenzene radical cation and a Co(II) center; this pathway is strongly supported by the femtosecond transient absorption spectra findings. No cooperation effects among the six azobenzene moieties in the photoisomerization process of $[\text{Co}^{\text{II}}(\text{dmAB})_3](\text{BF}_4)_2$ were

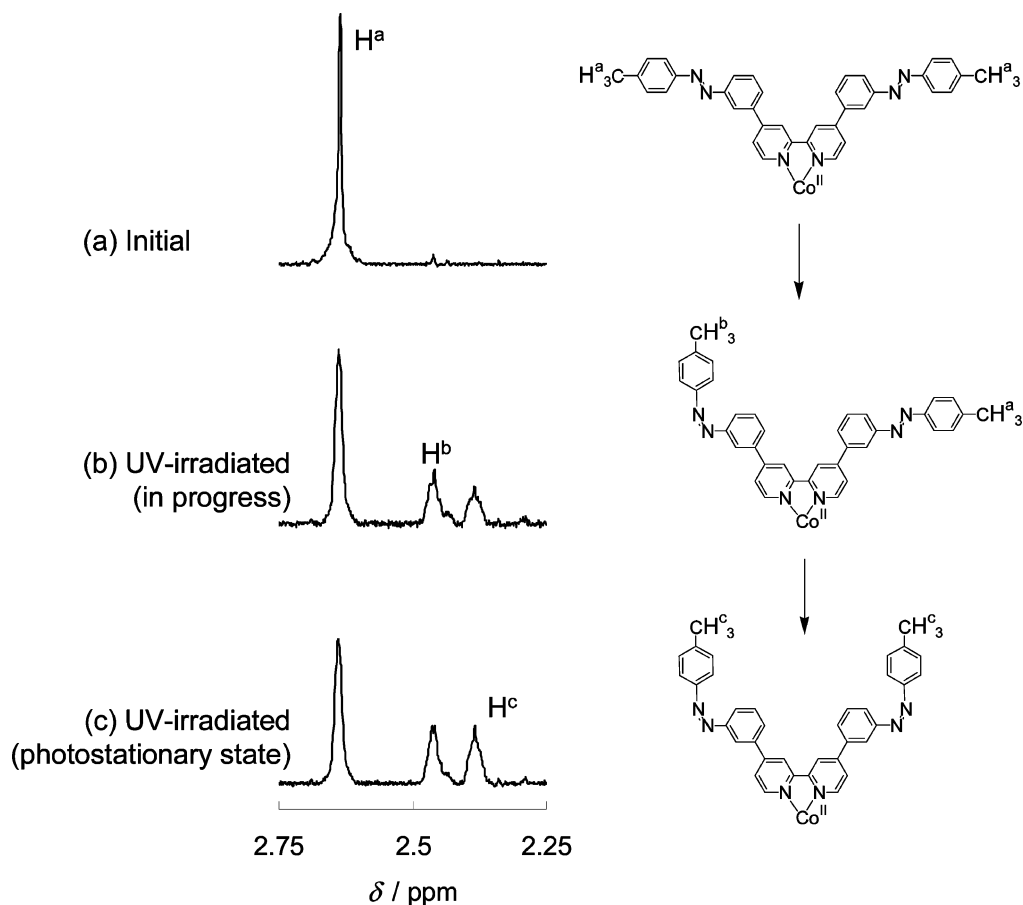


Figure 6. (left) ^1H NMR spectral changes of $[\text{Co}^{\text{II}}(\text{dmAB})_3](\text{BF}_4)_2$ upon UV irradiation in CD_2Cl_2 (400 MHz) and (right) aschematic representation of the stepwise photoisomerization, with the assignment of the methyl protons.

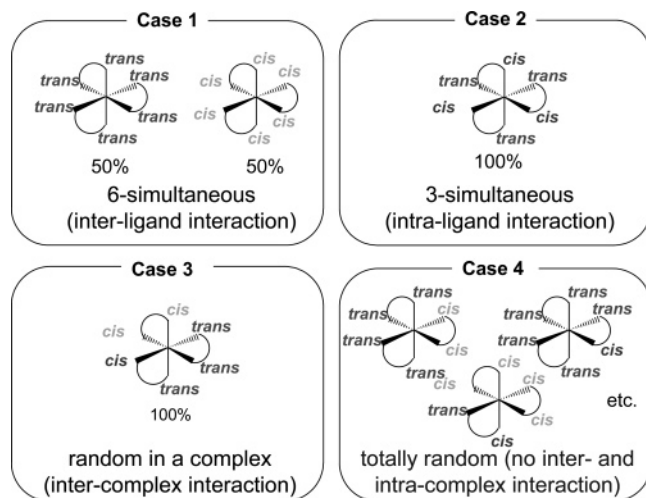


Figure 7. Schematic representation of possible cases of $[\text{Co}^{\text{II}}(\text{dmAB})_3](\text{BF}_4)_2$ in the PSS (50% cis).

observed according to the time-course changes in the ^1H NMR spectra. These results indicate the possibility of controlling the photoisomerization of several azobenzene moieties by the input and output of one electron at the metal center.

Experimental Section

Materials. 2-Acetylpyridinium iodide,²⁹ tetrakis(triphenylphosphine)palladium(0),³⁰ 4-nitrosotoluene,³¹ 2,2'-bipyridine-*N,N'*-

dioxide,³² 4,4'-dinitro-2,2'-bipyridine-*N,N'*-dioxide,³³ 4,4'-dibromo-2,2'-bipyridine-*N,N'*-dioxide,³⁴ and 4,4'-dibromo-2,2'-bipyridine³¹ were prepared according to methods reported in the literature.

All reagents were purchased from Kanto Kagaku Co., Ltd., except for sodium pyruvate, tetraethylammonium tetrafluoroborate, and 3-nitrobenzaldehyde (obtained from Tokyo Kasei Kogyo Co., Ltd.) and ammonium tetrafluoroborate, phosphorus tribromide, cobalt(II) nitrate, and cobalt(II) chloride (obtained from Wako Pure Chemical Industries, Ltd.).

Apparatus. The ^1H NMR spectra were measured with JEOL EX270, JEOL JNM-AL400, JEOL JNM-ECX400, and Bruker DRX 500 spectrometers. The UV–vis spectra were obtained with JASCO V-570 and Hewlett-Packard 8453 spectrometers. The ESI-TOF MS spectra and MALDI-TOF MS spectra were recorded with a Micromass-LCT spectrometer and a Shimadzu-Kratos AXIMA-CFR spectrometer, respectively. Cyclic voltammetry was carried out under an argon atmosphere in a standard one-compartment cell equipped with a glassy carbon rod (outside diameter 3 mm, Tokai Carbon GC-20), a platinum-wire counter electrode, and a Ag/Ag^+ reference electrode [10 mM AgClO_4 in 0.1 M *n*- $\text{Bu}_4\text{ClO}_4/\text{acetonitrile}$ solution, $E^0(\text{ferrocenium}/\text{ferrocene}) = 0.16$ V vs Ag/Ag^+] using a BAS CV-50W or an ALS 750A voltammetric analyzer.

(29) Krönke, F. *Synthesis* **1976**, 1, 1.

(30) Coulson, D. R. *Inorg. Synth.* **1972**, 13, 121.

(31) Hall, J. H.; Dolan, F. W. *J. Org. Chem.* **1978**, 43, 4608.

(32) Murase, I. *Nippon Kagaku Zasshi* **1956**, 77, 682.

(33) (a) Haginiwa, J. *Yakugaku Zasshi* **1955**, 75, 731. (b) Anderson, A.; Constable, E. C.; Seddon K. R.; Turp, J. E. *J. Chem. Soc., Dalton Trans.* **1985**, 2247.

(34) Maerker, G.; Case, F. H. *J. Am. Chem. Soc.* **1958**, 80, 2475.

Magnetic susceptibility data were obtained with an MPMS SQUID susceptometer (Quantum Design, Inc.), where the applied magnetic fields were 1 kOe. The photoirradiation experiments were performed with a super-high-pressure mercury lamp (USHIO-500D) as the light source, and each emission line (365 and 436 nm) was separated with a monochromator (JASCO CT-10T, $\Delta\lambda = \pm 30$ nm).

4,4'-Bis(3''-nitrophenyl)-2,2'-bipyridine (1). A solution of 4,4'-dibromo-2,2'-bipyridine (491 mg, 1.56 mmol) and Pd(PPh₃)₄ (135 mg, 0.117 mmol) in 8 mL of degassed toluene was combined with a solution of 3-nitrophenylboronic acid (673 mg, 4.03 mmol) and sodium carbonate (679 mg, 6.41 mmol) in 8 mL of a degassed 4:1 water/methanol solution.³⁵ The biphasic mixture was refluxed for 26 h under a nitrogen atmosphere, and the solution turned into a pale brown suspension. Another portion of Pd(PPh₃)₄ (45 mg, 0.039 mmol) was added to the suspension, and the mixture was refluxed for 17 h. The resulting suspension was cooled to room temperature. The resulting white powder of **1** was filtered and washed with water, toluene, and ether (570 mg, 89.8%). The product was used without further purification. ¹H NMR (CDCl₃): δ (ppm) 8.84 (d, 2H, $J = 4.9$ Hz), 8.81 (d, 2H, $J = 1.6$ Hz), 8.65 (s, 2H), 8.34 (dd, 2H, $J = 5.9, 2$ Hz), 8.13 (d, 2H, $J = 7.8$ Hz), 7.73 (dd, 2H, $J = 8.1, 8.1$ Hz), 7.63 (dd, 2H, $J = 4.9, 1.9$ Hz).

4,4'-Bis(3''-aminophenyl)-2,2'-bipyridine (2). The dinitro compound **1** (584 mg, 1.47 mmol) was suspended in hydrochloric acid (21 mL) and acetic acid (42 mL).³⁶ Tin(II) chloride dihydrate (6.67 g, 29.6 mmol) in water (31 mL) was added to the suspension, and then the suspension was refluxed. After 24 h, the light brown suspension turned into a light orange solution. The resulting solution was cooled to room temperature and basified to pH 11 with aqueous NaOH (25%). The pale brown precipitate of **2** was filtered and washed with water and methanol (442 mg, 89.1%). The product was used without further purification. ¹H NMR (CDCl₃): δ (ppm) 8.73 (d, 2H, $J = 4.9$ Hz), 8.67 (s, 2H), 7.53 (dd, 2H, $J = 5.4, 1.6$ Hz), 7.29 (dd, 2H, $J = 7.6, 7.6$ Hz), 7.17 (d, 2H, $J = 7.6$ Hz), 7.11 (s, 2H), 6.78 (d, 2H, $J = 9.2$ Hz), 3.82 (br, 4H).

4,4'-Bis(3''-(4'''-tolylazo)phenyl)-2,2'-bipyridine (dmAB). The diamino compound **2** (654 mg, 1.93 mmol) was dissolved in acetic acid (30 mL) and chloroform (30 mL).³⁷ 4-Nitrosotoluene (1.03 g, 8.46 mmol) was added to the solution, and the dark brown suspension was stirred at room temperature under a nitrogen atmosphere. Initially, the suspension turned black, and then it subsequently turned brown. After 26 h, another portion of 4-nitrosotoluene (660 mg, 5.45 mmol) was added to the suspension, which was stirred for an additional 24 h. The dark orange suspension was basified to pH 10 with aqueous NaOH (25%), and the product was extracted with chloroform. The combined organic layers were dried with sodium sulfate and evaporated. The residue was purified with alumina column chromatography. Nitrotoluene and nitrosotoluene were eluted with 30% chloroform/*n*-hexane, and then dmAB was eluted with 50–80% chloroform/*n*-hexane. Evaporation gave an orange solid (835 mg, 79.3%). ¹H NMR (CD₂Cl₂): δ (ppm) 8.89 (s, 2H), 8.80 (d, 2H, $J = 5.1$ Hz), 8.35 (dd, 2H, $J = 2.8, 2.8$ Hz), 8.01 (d, 2H, $J = 8.5, 1.0$ Hz), 7.93 (d, 2H, $J = 7.7$ Hz), 7.89 (d, 4H, $J = 8.2$ Hz), 7.68–7.71 (m, 4H), 7.38 (d, 4H, $J = 8.1$ Hz), 2.46 (s, 6H). MALDI-TOF MS: m/z calcd, 545.2 ([M + H]⁺); found, 545.7. Anal. Calcd for C₃₆H₂₈N₆·0.5H₂O: C, 78.10; H, 5.28; N, 15.18. Found: C, 78.01; H, 5.30; N, 15.01.

(35) Damrauer, N. H.; Boussie, T. R.; Devenney, M.; McCusker, J. K. *J. Am. Chem. Soc.* **1997**, *119*, 8253.

(36) Filer, C. N.; Granchelli, F. E.; Soloway, A. H.; Neumeyer, J. L. *J. Org. Chem.* **1978**, *43*, 672.

(37) Anpson, H. D. *Org. Synth.* **1945**, *25*, 86.

[Co^{II}(dmAB)₃](BF₄)₂·CoCl₂·6H₂O (10.0 mg, 0.0420 mmol) and dmAB (67.7 mg, 0.124 mmol) were stirred in 60 mL of dichloromethane for 14 h under a nitrogen atmosphere, and then the solution was evaporated. The residue was dissolved in 400 mL of methanol and filtered to remove insoluble impurities (dmAB) under a nitrogen atmosphere. To this solution was added a solution of NH₄BF₄ (1.90 g, 18.1 mmol) in 20 mL of water. The resulting solution was kept at –20 °C for 28 h. The orange precipitate thus produced was filtered and washed with water and methanol (18 mg, 23%). ¹H NMR (CD₂Cl₂): δ (ppm) 94.61 (br, 6H), 81.08 (s, 6H), 44.54 (s, 6H), 11.70 (s, 6H), 10.68 (s, 6H), 9.68 (d, 6H, $J = 7.6$ Hz), 8.30–8.35 (m, 18H), 7.59 (d, 12H, $J = 8.0$ Hz), 2.64 (s, 18H). ESI-MS: m/z calcd, 846.32 ([Co(C₃₆H₂₈N₆)₃]²⁺); found, 846.30. Anal. Calcd for [Co(C₃₆H₂₈N₆)₃](BF₄)₂·2H₂O: C, 68.18; H, 4.66; N, 13.25. Found: C, 68.83; H, 4.90; N, 12.79.

[Co^{III}(dmAB)₃](BF₄)₃·Co(NO₃)₂·6H₂O (24.8 mg, 0.0852 mmol) and dmAB (135 mg, 0.247 mmol) were stirred in 9 mL of dichloromethane for 45 h under a nitrogen atmosphere. The initially yellow solution turned orange. AgCF₃SO₃ (87.5 mg, 0.341 mmol) was added to the solution. After the solution had been stirred for 4.5 h, a brown precipitate was formed. The solvent was removed by evaporation, and the residue was dried under reduced pressure. The residue was dissolved in methanol (250 mL), and then the solution was filtered in air to remove the Ag powder. To the filtrate was added 17 mL of aqueous NH₄BF₄ (1.70 g, 16.2 mmol). An orange precipitate was collected by filtration, and the filtrate was purified by reprecipitation from acetonitrile/ether and dichloromethane/ether (28.1 mg, 16.9%). ¹H NMR (CD₂Cl₂): δ (ppm) 9.06 (d, 6H, $J = 2.0$ Hz), 8.45 (dd, 6H, $J = 1.8, 1.8$ Hz), 8.23 (dd, 6H, $J = 6.3, 2.0$ Hz), 8.10–8.16 (m, 12H), 7.79–7.87 (m, 24H), 7.32 (d, 12H, $J = 8.2$ Hz), 2.43 (s, 18H). ESI-MS: m/z calcd, 564.21 ([Co(C₃₆H₂₈N₆)₃]³⁺); found, 564.23. Anal. Calcd for [Co(C₃₆H₂₈N₆)₃](BF₄)₃·2H₂O: C, 65.21; H, 4.46; N, 12.67. Found: C, 65.13; H, 4.49; N, 12.11.

4-(3''-Nitrophenyl)-2,2'-bipyridine (3). A mixture of 3-(3'-carboxy-3'-oxo-1'-propenyl)nitrobenzene (4.0 g, 18 mmol), 2-acetylpyridinepyridinium iodide (5.9 g, 18 mmol), and ammonium acetate (20 g, 0.26 mol) in water (100 mL) was refluxed for 2.5 h.¹⁵ The resulting solution was cooled to room temperature. A light gray solid of 4-(3''-nitrophenyl)-6-carboxy-2,2'-bipyridine was filtered, washed with water, and dried under reduced pressure. Quinoline (7 mL) was added to the product, and the mixture was heated at 150–160 °C for 7 h. Then, the excess quinoline was removed under reduced pressure at 150 °C. The black residue was purified by alumina column chromatography. The first pale yellow band eluted with CHCl₃ was collected. A white solid of **3** was obtained after the solvent had been removed (2.5 g, 50%). ¹H NMR (CDCl₃): δ (ppm) 8.80 (d, 1H, $J = 4.9$ Hz), 8.73 (m, 2H), 8.62 (s, 1H), 8.48 (d, 1H, $J = 8.4$ Hz), 8.32 (d, 1H, $J = 7.3$ Hz), 8.10 (d, 1H, $J = 7.8$ Hz), 7.86 (td, 1H, $J = 7.6, 1.6$ Hz), 7.70 (t, 1H, $J = 8.1$ Hz), 7.57 (dd, 1H, $J = 5.4, 1.6$ Hz), 7.36 (ddd, 1H, $J = 7.3, 4.6, 1.2$ Hz).

4-(3-Aminophenyl)-2,2'-bipyridine (4). Compound **3** (2.5 g, 8.9 mmol) was dissolved in concentrated HCl (20 mL).³⁸ A suspension of SnCl₂·2H₂O (9.0 g, 40 mmol) in water (60 mL) was added dropwise into the solution over a period of 30 min. The solution was stirred for 3 h at room temperature, and then another portion of SnCl₂·2H₂O (4.0 g, 18 mmol) in water (20 mL) was added over a period of 5 min. The suspension was heated to 100 °C for 2.5 h. Then another portion of concentrated aqueous HCl (20 mL) was added to the suspension, and the reaction was continued for 1 h. The reaction mixture was basified with NaOH (40 g). The product

(38) Hodgson, H. H.; Smith, E. W. *J. Chem. Soc.* **1935**, 671.

of **4** was extracted with ethyl acetate, and the solvent was removed by evaporation. Recrystallization from EtOH gave pale brown crystals (1.3 g, 60%). $^1\text{H NMR}$ (CDCl_3): δ (ppm) 8.71 (m, 2H), 8.63 (d, 1H, $J = 1.1$ Hz), 8.45 (d, 1H, $J = 7.8$ Hz), 7.84 (td, 1H, $J = 7.8, 1.9$ Hz), 7.51 (dd, 1H, $J = 5.4$ Hz, 2.2 Hz), 7.33 (dd, 1H, $J = 7.6, 5.1$ Hz), 7.28 (t, 1H, $J = 7.6$ Hz), 7.15 (d, 1H, $J = 7.8$ Hz), 7.09 (s, 1H), 6.77 (d, 1H, $J = 7.8$ Hz). Anal. Calcd for $\text{C}_{16}\text{H}_{13}\text{N}_3$: C, 77.71; H, 5.30; N, 16.99. Found: C, 77.46; H, 5.32; N, 17.00.

4-[3''-(4'''-Tolylazo)phenyl]-2,2'-bipyridine (mAB). To a solution of **4** (740 mg, 3.0 mmol) in acetic acid (10 mL) was added 4-nitrosotoluene (1.0 g, 8.3 mmol) portionwise over 20 h until the aniline derivative disappeared.³⁹ The dark orange solution was neutralized with NaOH (3.9 g), and the products were extracted with CHCl_3 . The residue was purified with alumina column chromatography. Nitrotoluene and nitrosotoluene were eluted with CHCl_3 /hexane (1:2 v/v), and then mAB was eluted with CHCl_3 . Recrystallization from EtOH gave orange crystals (320 mg, 31%). $^1\text{H NMR}$ (CDCl_3): δ 8.77 (d, 1H, $J = 3.0$ Hz), 8.76 (s, 1H), 8.73 (d, 1H, $J = 7.6$ Hz), 8.48 (d, 1H, $J = 8.1$ Hz), 8.31 (s, 1H), 7.99 (d, 1H, $J = 7.8$ Hz), 7.89–7.82 (m, 3H), 7.65 (t, 1H, $J = 7.6$ Hz), 7.64 (d, 1H, $J = 4.9$ Hz), 7.37–7.32 (m, 2H), 2.46 (s, 3H). Anal. Calcd for $\text{C}_{23}\text{H}_{18}\text{N}_4$: C, 78.83; H, 5.18; N, 15.99. Found: C, 78.73; H, 5.20; N, 16.01.

[Co(mAB)₃](BF₄)₂. Under a nitrogen atmosphere, $\text{Co}(\text{NO}_3)_2 \cdot 6\text{H}_2\text{O}$ (19 mg, 0.065 mmol), mAB (70 mg, 0.20 mmol), and tetraethylammonium tetrafluoroborate (1 g, 5 mmol) were stirred in CH_2Cl_2 (20 mL) for 8 h. The solvent was removed under reduced pressure, and the residue was washed with water, dissolved in 20 mL of dichloromethane, and filtered off. A yellow powder was formed by the addition of ether (40 mL) to the filtrate, and the product was collected by filtration in air (64 mg, 85%). Anal. Calcd for $\text{C}_{69}\text{H}_{54}\text{B}_2\text{CoF}_8\text{N}_{12} \cdot 2\text{H}_2\text{O}$: C, 62.79; H, 4.43; N, 12.73. Found: C, 62.91; H, 4.77; N, 12.82.

[Co(mAB)₃](BF₄)₃. Under a nitrogen atmosphere, $\text{Co}(\text{NO}_3)_2 \cdot 6\text{H}_2\text{O}$ (19 mg, 0.065 mmol) and mAB (70 mg, 0.20 mmol) were stirred in CH_2Cl_2 (20 mL) for 10 h. AgCF_3SO_3 (65 mg, 0.25 mmol) was added to the red solution. After the solution was stirred for 14 h, an orange precipitate formed. The solvent was removed by evaporation, and the residue was dried under reduced pressure, dissolved in methanol (30 mL), and filtered to remove the Ag powder. To the filtrate was added 10 mL of aqueous NH_4BF_4 (2.0 g, 20 mmol). The orange precipitate was collected by filtration and purified by reprecipitation from acetonitrile/ether (79 mg, 89%). Anal. Calcd for $\text{C}_{69}\text{H}_{54}\text{B}_3\text{CoF}_{12}\text{N}_{12} \cdot 3\text{H}_2\text{O}$: C, 58.17; H, 4.24; N, 11.80. Found: C, 58.11; H, 4.27; N, 11.62. $^1\text{H NMR}$ ($\text{DMSO}-d_6$):

δ 9.54 (s, 3H), 9.50–9.40 (m, 3H), 8.72–8.60 (m, 3H), 8.58 (s, 3H), 8.30–8.20 (m, 6H), 8.12 (d, 3H, $J = 7.6$ Hz), 7.95–7.80 (m, 6H), 7.85 (d, 6H, $J = 8.4$ Hz), 7.75–7.40 (m, 6H), 7.45–7.38 (m, 9H), 2.43 (s, 9H).

Femtosecond Time-Resolved Absorption Spectroscopy. The protocol for the femtosecond pump–probe experiment was essentially the same as that reported in the literature.⁴⁰ Briefly, the laser system consisted of a hybrid mode-locked, dispersion-compensated femtosecond dye laser (Coherent, Satori 774) and a dye amplifier (Continuum, RGA 60-10 and PTA 60). The dye laser (gain dye Pyridine 2 and saturable absorber DDI) was pumped with a cw mode-locked Nd:YAG laser (Coherent, Antares 76S). The sample was excited by the second harmonic (360 nm) of the fundamental (center wavelength, 720 nm; pulse width, ~ 200 fs fwhm) at a repetition of rate of 10 Hz. The residual portion of the fundamental output was focused on a 1-cm H_2O cell to generate a femtosecond supercontinuum probe pulse. The planes of polarization of the pump and probe beams were set to the magic angle (54.7°) to avoid any anisotropic contribution to the transient signal. Both of the beams were focused on the sample in a 2-mm cuvette at an angle of less than 5° . Transient absorption spectra were obtained by averaging over 200 pulses, and these spectra were analyzed by an intensified multichannel detector (Princeton Instruments, ICCD-576) as a function of the probe-delay time. The spectra were corrected for the intensity variations and time dispersions of the supercontinuum. The sample solution was allowed to flow through a 2-mm flow cell using a magnetically coupled gear pump (Micropump, 040-332) to avoid any possibility of sample damage during the measurement of transient absorption.

Acknowledgment. This work was supported by Grants-in-Aid for Scientific Research [Nos. 16047204 (area 434) and 17205007] and by a grant from the 21st Century COE Program for Frontiers in Fundamental Chemistry from MEXT, Japan.

Supporting Information Available: Schemes for the syntheses of the compounds (Schemes S1 and S2), results of single-crystal X-ray diffraction analysis of dmAB (Figure S1 and Table S1), UV–vis absorption spectra of the ligands and related compounds (Figures S2 and S3), cyclic voltammograms of $[\text{Co}^{\text{III}}(\text{dmAB})_3](\text{BF}_4)_3$ (Figure S4), molar magnetic susceptibility data for $[\text{Co}^{\text{II}}(\text{dmAB})_3](\text{BF}_4)_2$ (Table S2), and $^1\text{H NMR}$ spectra of the ligands and complexes before and after UV irradiation (Figures S5–S9). These materials are available free of charge via the Internet at <http://pubs.acs.org>.

IC0513538

(39) Schmitt, C. C.; Moritz, C. A.; Pizzolatti, M. G.; Yunes, R. A. *Bull. Chem. Soc. Jpn.* 1989, 62, 3684.

(40) (a) Tamai, N.; Masuhara, H. *Chem. Phys. Lett.* 1992, 191, 189. (b) Mitram, S.; Tamai, N. *Chem. Phys. Lett.* 1998, 282, 391.